NJC

Accepted Manuscript

This is an *Accepted Manuscript*, which has been through the Royal Society of Chemistry peer review process and has been accepted for publication.

Accepted Manuscripts are published online shortly after acceptance, before technical editing, formatting and proof reading. Using this free service, authors can make their results available to the community, in citable form, before we publish the edited article. We will replace this *Accepted Manuscript* with the edited and formatted *Advance Article* as soon as it is available.

You can find more information about *Accepted Manuscripts* in the Information for Authors.

Please note that technical editing may introduce minor changes to the text and/or graphics, which may alter content. The journal's standard Terms & Conditions and the Ethical guidelines still apply. In no event shall the Royal Society of Chemistry be held responsible for any errors or omissions in this *Accepted Manuscript* or any consequences arising from the use of any information it contains.

ROYAL SOCIETY OF CHEMISTRY

www.rsc.org/njc

Journal Name

ARTICLE

Fully conjugated block copolymers for single-component solar cells: synthesis, purification, and characterization†

Received 00th January 20xx,
Accepted 00th January 20xx

DOI: 10.1039/x0xx00000x

www.rsc.org/

Shifan Wang,[a] Qingqing Yang,[b] Youtian Tao,*[a] Yan Guo,[c] Jie Yang,[a] Yanan Liu,[a] Lingyun Zhao,[a] Zhiyuan Xie,*[b] Wei Huang*[a]

Fully conjugated donor-acceptor (D-A) block copolymers, P3HT-*b*-PBIT2, containing *p*-type poly(3-hexylthiophene) and *n*-type poly(pyrene bismide) segments are synthesized in a one-pot reaction *via* Stille coupling polycondensation. Various D-A block copolymers with low polydispersities (1.17-1.54) are obtained through further separation by preparative GPC. The structural and molecular features of block copolymers are verified by ^{1}H NMR, fourier transform infrared spectroscopy (FTIR), UV-Vis absorption, and cyclic voltammetry (CV). It is found that optical and electrochemical properties of D-A block copolymers are strongly dependent on the combination ratio of the donor P3HT and acceptor PBIT2 segment. When PBIT2 weight content increases, the absorption intensity of PBIT2 in D-A block copolymer fractions enhances simultaneously. The highest occupied molecular orbital (HOMO) levels of the block copolymers increase gradually with decreasing the acceptor block lengths and are located between P3HT and PBIT2. All-polymer solar cells using the preparative GPC separated P3HT-*b*-PBIT2 (BCP1-1) as single-component active layer, which shows mono-mondal GPC curves and comparatively balanced hole and electron mobility of 2.36×10^{-4} and 1.15×10^{-5} cm^2/V s respectively, achieve a power conversion efficiency of 1.0% with open-circuit voltage of 0.43 V, short-current of 5.29 mA/cm^2, and fill factor of 0.43.

Introduction

All-polymer solar cells continue to attract considerable attention in recent years for their potential to supplant polymer/fullerene devices,[1–5] because the polymer/polymer blends allow for covering the complementary parts of the solar spectrum by tuning the energy levels of each component.[6] However, the power conversion efficiencies (PCEs) of the all-polymer solar cells are generally lagging far behind that of the fullerene-based organic solar cells. One of the critical issues account for the poor efficiency is undesirable morphological characteristics of the polymer blends, such as poor crystallinity,[7] inhomogeneous internal phase composition,[8–10] and a large-scale phase separation.[11–13] Controlling phase separation is a key issue in all-polymer solar cells which limits the generation of free charge carriers and subsequently influences the device performance.[14] The nanoscale phase-separated active layer with interpenetrating networks in solar cell devices may provide high interfaces which ensure efficient exciton dissociation and charge transport.[15-17] Diverse methods have been used to optimize nanoscale phase separation, including thermal annealing, solvent vapor annealing, and the use of processing additives.[18-21] However, limited success has been achieved in all-polymer solar cells.[22]

Block copolymers consisting of covalently linked donor and acceptor blocks constitutionally prefer composition-dependent nanoscale phase separation.[6,14,23-25] Phase-separated donor and acceptor block copolymers are expected to address current challenges in morphology manipulation.[26] For example, our group previously reported the all-conjugated block copolymers P3HT-*b*-PNDT films showing significant fine structures and much smoother film morphologies than P3HT/PNDIT homopolymer blends.[27] Hawker *et al*. also proposed a strategy for the synthesis of fully conjugated donor-acceptor block copolymers P3HT-*b*-DPP, which provided a rich self-assembly behaviour with two separate crystalline domains.[28] Power conversion efficiency up to 3% was realized by using P3HT-*b*-PFTBT block copolymer as the active layer, demonstrating efficient photo conversion well beyond devices composed of P3HT/PFTBT homopolymer blends.[29] Up to date, research on the fully conjugated donor-acceptor block copolymers have been rarely reported.[27-36] A critical component in the execution of this approach is the choice of architecture for the D-A block copolymer. Ideally, the individual blocks of the D-A block copolymer should contain chromophoric units with appropriately aligned the HOMO and the lowest unoccupied molecular orbital (LUMO) energy levels to make it possible to elicit a photovoltaic response when the two materials are combined.[37] Starting from these facts,

[a] Key Laboratory of Flexible Electronics & Institute of Advanced Materials, Jiangsu National Synergistic Innovation Center for Advanced Materials (SICAM), Nanjing Tech University, 30 South Puzhu Road, Nanjing 211816, China
[b] Changchun Institute of Applied Chemistry, Chinese Academy of Sciences, 5625 Renmin Street, Changchun, 130022, China.
[c] Department of Biomedical Engineering, College of Engineering and Applied Sciences, Nanjing University, Nanjing, Jiangsu 210093, China
†Electronic Supplementary Information (ESI) available: ^{1}H NMR spectra. See DOI: 10.1039/x0xx00000x

several studies of D-A non-conjugated block copolymers comprising regioregular P3HT donor blocks and pyrene bismide (PBI) acceptor blocks have been reported in which PBI functionalized as side chain hanging in the non-conjugated polyethylene backbone.[37-44] P3HT is one of the most effective *p*-type materials used in solar cells; PBI is an *n*-type electron compound with excellent electron mobility up to 10^{1}-10^{-3} cm^2/ V s^{45-50}, and it also displays a favourable energy level offset with respect to that of P3HT, ensuring that photoinduced electron transfer can take place from the donor block to the acceptor block.[51] Devices based on *rr*P3HT-*b*-poly(perylene bisimide acrylate) copolymer as single-component active layers in OPVs exhibited PCEs of 0.49%,[38] while devices based on P3HT-*b*-PPerAcr which comprised of a P3HT donor block coupled to a poly(perylene bisimide acrylate), gave a PCE of 0.35%.[42] Nevertheless, there has not been report on fully conjugated block copolymers with P3HT as donor blocks and PBI as acceptor blocks in which a conjugated linkage is connected through P3HT and PBI.

Herein, we present the synthesis, purification and characterization of all-conjugated block copolymers, comprising P3HT donor and PBIT2 acceptor block. After careful purification with preparative GPC, the structure, optical and electrochemical properties, and film morphologies of the newly purified fully conjugated copolymers have been investigated in detail. All-polymer solar cells using the purified P3HT-*b*-PBIT2 as single-component active layer achieved a power conversion efficiency of 1.0% with open-circuit voltage of 0.43 V, short-current of 5.29 mA/cm^2, and fill factor of 0.43.

Experimental section

Materials

All reagents were purchased from Energy Chemical, Suna Tech Inc, Stream, Sigma Aldrich and used without further purification. Reagent grade solvents used in this study were freshly dried using standard distillation methods, except *N,N*-dimethylformamide (DMF) was purchased from Sigma-Aldrich.

Characterization

^{1}H NMR spectra were measured on a Bruker DRX-400 spectrometer. Elemental analyses of carbon, hydrogen, and nitrogen were performed on a Vario EL III microanalyzer. Number-average (M_n) and Weight-average (M_w) of all polymers were determined by Agilent Technologies 1200 series GPC running in chlorobenzene at 80°C, using two PL mixed B columns in series, and calibrated against narrow polydispersity polystyrene standards. Preparative GPC utilized a Shimadzu recycling GPC system running in chlorobenzene at 80°C, using Agilent PL gel MIXED-D column, DGU-20A3 Degasser, LC-20A Pump, CTO-20A Column Oven andSPD-20A UV Detector. The ultraviolet-visible (UV-Vis) absorption spectra were recorded on a Shimadzu UV-2500 recording spectrophotometer. Fourier transform infrared spectroscopy (FTIR) measurements were performed on a Nicolet 6700 spectrometer equipped with a MCT detector. Cyclic voltammetry (CV) was measured on a CHI660D electrochemical workstation with a solution of 0.1 mol/L tetrabutylammonium hexafluorophosphate (Bu_4NPF6) in acetonitrile, and the polymer film on a Pt plate as the working electrode, a platinum wire as auxiliary electrode, and an Ag wire as pseudo-reference electrode with ferrocenium-ferrocene (Fc^+/Fc) as the internal standard. The scan rate was 100 mV/s. Atomic force microscopy (AFM) was conducted on SPA300HV in tapping mode using an SPI3800 controller, Seiko Instruments Industry, Co., Ltd. The X-ray diffraction (XRD) study of the samples is carried out on a Bruker D8 Focus X-ray diffractometer operating at 30 kV and 20 mA with a copper target (l = 1.54 Å) and at a scanning rate of 1° min^{-1}.

Device fabrication and measurements

The polymer solar cells have a structure of indium tin oxide (ITO)-coated glass substrate /PEDOT:PSS/actively layer/Ca/Al. Poly(ethylenedioxythiophene):poly(styrenesulfonate)(PEDOT:PSS) (Baytron P4083) was firstly spin-coated on the pre-cleaned ITO substrate to produce a 35-nm-thick anode buffer layer. The 85 nm thick active layer with a concentration of 10 mg/mL in chlorobenzene solution was spin-coated onto the PEDOT:PSS layer. The samples were then transferred into a vacuum evaporator and a cathode including 5 nm of Ca and 100 nm Al was thermally deposited on top of the active layer to produce an active area of 0.12 cm^2 for each device. Devices with thermal annealing were carried out in a glove box at 150°C for 10 min. The thicknesses of the polymer blend films were determined with a DEKTAK 6M Stylus profile meter (Bruker, Germany). The illuminated J-V characteristics of the solar cells were measured under a nitrogen atmosphere using a computer-controlled Keithley 236 source meter (Keithley Instruments Inc., USA) under 100 mW/cm^2 AM1.5G simulated solar-light illumination. The light intensity was determined by a calibrated silicon diode with a KG-5 visible color filter. External quantum efficiencies (EQE) were determined at room temperature using a 75 W Xe lamp source as excitation light and a 150 W quartz-tungsten-halogen lamp (QE-R, Enli Technology Co. Ltd., Taiwan, China) for background illumination. Hole-only or electron-only diodes were fabricated using the architecture of ITO/PEDOT:PSS/active layer/Au for holes and Al/active layer/Al for electrons. Mobilities were extracted by fitting the current density–voltage curves using the Mott–Gurney relationship (space charge limited current).

Synthesis

PBIT2 A mixture of 5,5'-bis(trimethylstannyl)-2,2'-bithiophene (59.0 mg, 0.12 mmol), *N*,*N*'-Bis(2-decyl-tetradecyl)-1,7-dibromo-3,4,9,10-perylene diimide (146.6 mg, 0.12 mmol), $Pd(PPh_3)_4$ (6.0 mg, 0.0048 mmol) was placed in a 10 mL Schlenk tube and degassed with nitrogen. Dry toluene (1.9 mL) and DMF (0.5 mL) were injected into the Schlenk tube. The mixture was heated at 120°C for 12 h. After cooling to room temperature, the mixture was poured into methanol, and the resulting precipitate was filtered. The raw polymer was purified by subsequent Soxhlet extraction with methanol, acetone, and chloroform as final solvent. The chloroform

fraction was precipitated from cold methanol again. After drying, 135 mg of dark solid was collected (92%). ^{1}H NMR

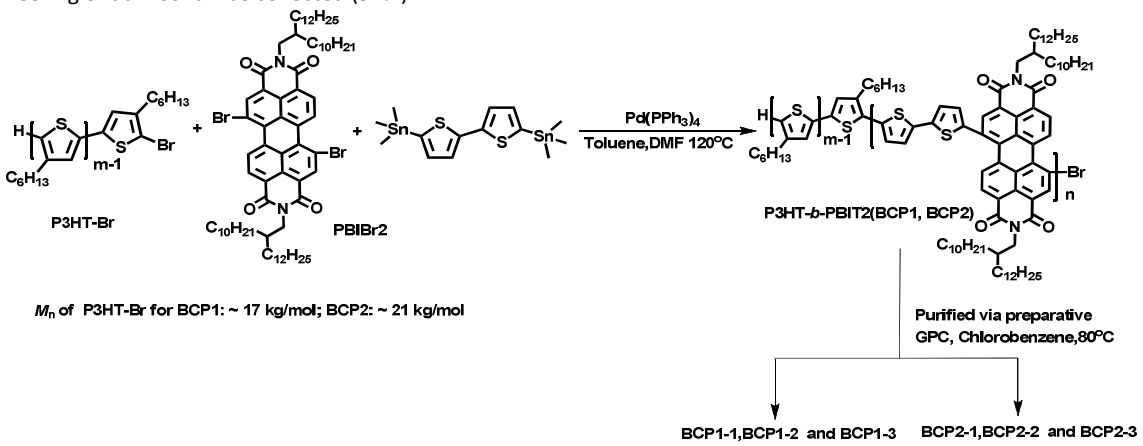

Scheme 1 Synthesis of block copolymer P3HT-*b*-PBIT2 in a one-pot reaction step. BCP1 and BCP2 were further purified *via* preparative GPC to obtain various D-A block copolymers with different Mn.

($CDCl_3$, 400 MHz) δ 8.73 (br, 2H), 8.40 (br, 4H), 8.30 (br, 2H), 7.09 (br, 2H), 4.13 (br, 4H), 2.02 (br, 2H), 1.25-1.19 (br, 62 H), 0.84 (br, 14H); GPC M_n = 9801 g/mol, M_w = 15026 g/mol, PDI = 1.53.

General procedure of block copolymer P3HT-*b*-PBIT (BCP1). A mixture of P3HT-1 (M_n = 17 kg/mol) (110.0 mg, ~0.007 mmol), 5,5'-bis(trimethylstannyl)-2,2'-bithiophene (98.4 mg, 0.200 mmol), *N*,*N*'-Bis(2-decyl-tetradecyl)-1,7-dibromo-3,4,9,10-perylene diimide (224.3 mg, 0.200 mmol), $Pd(PPh_3)_4$ (10.0 mg, 0.008 mmol) was placed in a 20 mL Schlenk tube and the atmosphere was replaced with nitrogen. Dry toluene (5 mL) and DMF (1 mL) were injected into the Schlenk tube, and then heated at 120°C for 12 h. After cooling to room temperature, the mixture was poured into methanol, and the resulting precipitate was filtered off and purified by subsequent Soxhlet extraction with methanol, acetone, ethyl acetate, and chloroform as final solvent. The chloroform fraction was precipitated from cold methanol again. After drying, a dark solid with a yield of 280 mg was collected. GPC M_n = 11219 g/mol, M_w = 17361 g/mol, PDI = 1.55.

BCP2 was prepared following the similar procedure with BCP1-1, by using 168 mg (~0.008 mmol) of P3HT-2 (M_n = 21 kg/mol), the crude product of a dark solid with a yield of 290 mg was collected. GPC M_n = 13353 g/mol, M_w = 21132 g/mol, PDI = 1.58.

Results and discussion

Synthesis and characterization

As outlined in scheme 1, P3HT-Br was synthesized and purified following our previous report.[27] The two new copolymers BCP1 and BCP2 were synthesized by Stille coupling polymerization of P3HT-Br, PBIBr2 and 5,5'-bis(trimethylstannyl)-2,2'-bithiophene in good yields, using $Pd(PPh_3)_4$ as catalyt. After reaction, the crude products were purified *via* Soxhlet extraction with methanol, acetone, ethyl acetate, and chloroform in succession. Molecular weight and polydispersity of all polymers were measured by GPC with chlorobenzene as the eluant and calibration against polystyrene standards. The number average molecular weights (M_n) of BCP1 and BCP2 were obtained to be 11.2 and 13.4 kg/mol, with PDIs of 1.55 and 1.58, respectively. Both polymers were fully soluble in common chlorinated organic solvents at room temperature, such as chloroform, chlorobenzene, *o*-dichlorobenzene.

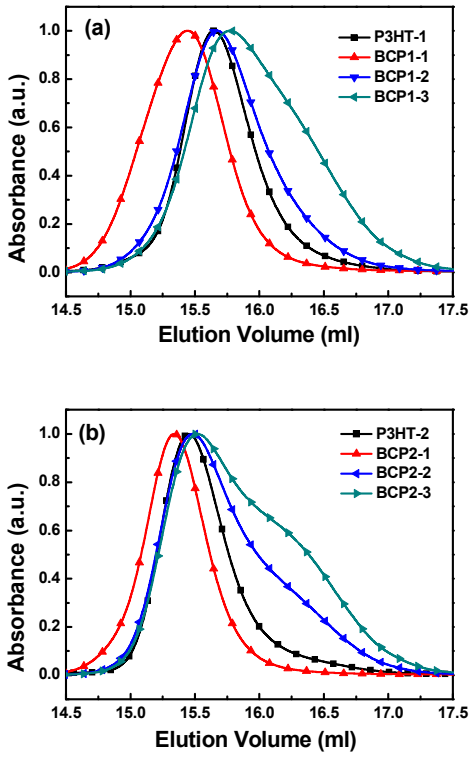

Fig. 1 GPC analysis of various block copolymer fractions purified by preparative GPC, with P3HT chain length of (a) 16.9 and (b) 21.2 kg/mol.

However, this method is not flawless, contamination with P3HT homopolymers is feasible, and hence tedious purification is necessary. In order to obtain the low polydispersity block copolymers, BCP1 and BCP2 were further purified *via* preparative GPC with chlorobenzene as eluent at 80°C. Both block copolymers were separated into six to seven parts, and only the effective three segments (BCP1-1, BCP1-2, BCP1-3, BCP2-1, BCP2-2 and BCP2-3) for each BCP were chosen for further investigation, the detail purification method can be found in previous report by Sommer et.al.[30] Molecular weight and polydispersity for all polymers are summarized in Table 1. Figure 1 shows the GPC curves of all selected block copolymers obtained from BCP1 and BCP2. It is obvious that GPC curves of all fractions with low polydispersitie are different from P3HT-1 in Figure 1a and P3HT-2 in 1b. It should be noted that block copolymers were not purified effectively *via* preparative GPC. However, BCP1-1 and BCP2-1 show sharp and monomodal profile, which is clearly shifted to shorter elution times compared to P3HT.

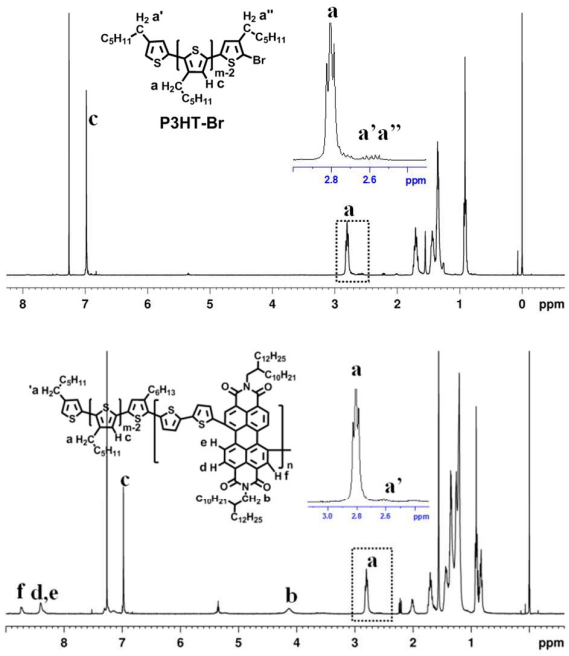

Fig. 2 ^{1}H NMR spectra for P3HT-Br (top) and the representative block copolymer BCP1-1(bottom).

According to the ^{1}H NMR spectra of P3HT-Br and BCP1-1 (Figure. 2), two specific peaks matching to the aromatic rings of PBIT2 were observed at 8.40 and 8.73 ppm. ^{1}H NMR spectroscopy shows distinct resonances for both the P3HT and PBI units, and the disappearance of peaks about 2.50 ppm resulting from the linkage between the bromo-chain end of the P3HT block and PBIT2 segment.[28,33] P3HT weight ratio was determined by comparing the integral area of the branched chain peak (4.13 ppm) from the PBI and the branched chain peak (2.80 ppm) of P3HT, and also could be calculated from the integration of the aromatic rings of the PBIT2 and P3HT segment (i.e., δ 8.73 and 6.98). Weight ratio of P3HT was basically averaged by branched chain and aromatic rings peak integral area. Thus various block copolymers with different P3HT weight rate were investigated and summarized in Table 1, and further confirmed by FTIR spectra.

Table 1 Molecular weights and polydispersity determined from GPC of various polymeric materials investigated in this work, and weight ratio of P3HT in block copolymers.

Sample	M_n (kg/mol)	M_w (kg/mol)	PDI	wt% P3HT[a]
PPBIT2	9.8	15.0	1.53	-
P3HT-1	16.9	20.2	1.19	-
BCP1-1	25.2	31.0	1.23	47
BCP1-2	15.4	20.1	1.30	46
BCP1-3	11.0	15.9	1.44	35
P3HT-2	21.2	25.4	1.20	-
BCP2-1	28.3	33.0	1.17	75
BCP2-2	15.0	21.7	1.45	51
BCP2-3	12.3	19.9	1.54	43

[a] Determined from the ^{1}H NMR.

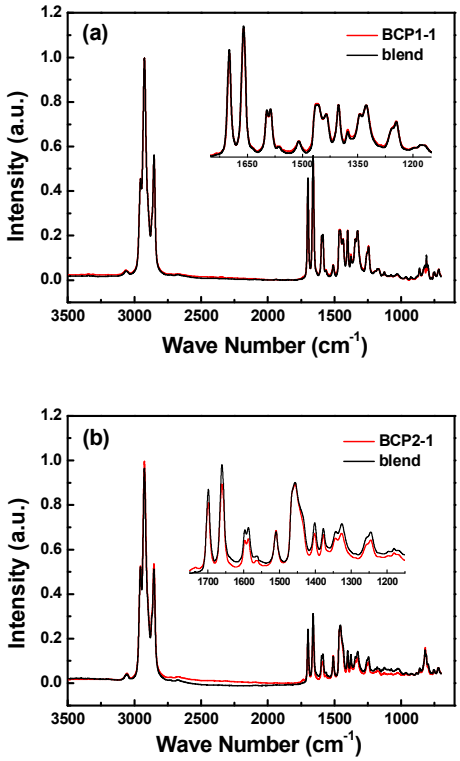

Fig. 3 Room temperature FTIR spectra of selected block polymers and D/A homopolymer blends with the same P3HT weight ratio calculated from the ^{1}H NMR. Inset: the enlarged spectra with wave number ranging from 1750-1150 cm^{-1}.

To access the structural and molecular characteristic of the block copolymers, and further to verify the weight ratio of P3HT in block copolymers calculated from ^{1}H NMR spectra, FTIR was carried out. As shown in Figure 3, the spectra of block copolymers P3HT-*b*-PBIT2 and P3HT/PBIT2 polymer blends are

almost identical, with exactly similar absorption peak and intensities because of the same chemical bonding component. From the fingerprint region for all the two groups of block copolymer and polymer blends, it is found that their spectra overlap very well, indicating the weight ratio of P3HT in block copolymers are similar with those in P3HT/PBIT2 polymer blends, respectively. The 1700 and 1663 cm^{-1} bands are corresponding to the C=O symmetric and anti-symmetric stretching bands of PBI,[52] and the ~1510 cm^{-1} corresponding to the C=C stretching band of the main chain of polythiophene.[53]

Optical properties

UV-Vis absorption spectra of the synthesized block copolymers, P3HT and PBIT2 homopolymers in chloroform solutions and thin films are showed in Figure 3 and related data are summarized in Table 2. In the dilute solution, all block copolymers exhibited similar absorption behaviour with a broad absorption in the visible regions. The absorption spectra of bock copolymers have demonstrated both of the P3HT and PBIT2 absorption features and are almost the overlap of the two component, indicating the deficit of ground state electronic interactions as expected.[54] Obviously, the absorption intensity depends on the chain length of the donor P3HT and acceptor PBIT2 segment. When PBIT2 weight content increases, the absorption intensity of PBIT2 in D-A block copolymer fractions gradually enhances simultaneously. In the film state, all bock copolymers exhibit similar absorption profiles with a broad absorption peaks from 300 to 800 nm, as well as significant red-shift for the longer wavelength absorption compared in solution, suggesting there might be certain molecular self-organization and highly ordered structures in the film which could facilitate charge transfer for photovoltaic application.[55-57] The optical band gaps of each bock copolymer calculated from the onset of the film absorption spectra are 1.6 ~ 1.8 eV, which are located in between the homopolymer P3HT and PBIT2.

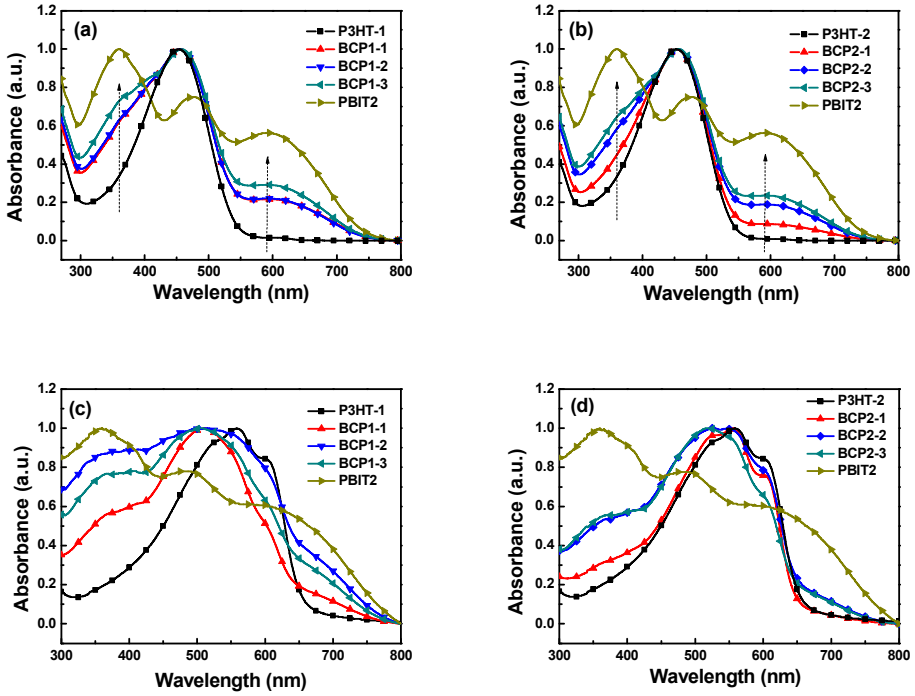

Fig. 4 UV-Vis absorption spectra of selected effective block polymer fractions, P3HT and PBIT2 homopolymers in $CHCl_3$ solution (a, b) and film state (c, d).

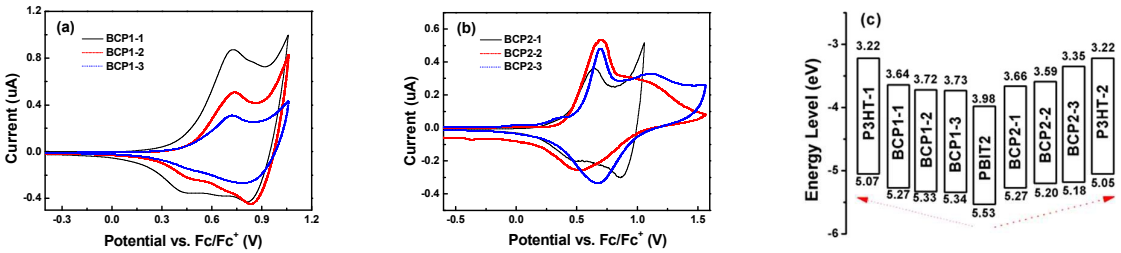

Fig. 5 Cyclic voltammogram of the block copolymers (a) BCP1 and (b) BCP2, (c) energy level diagram of block copolymers, P3HT and PBIT2.

Electrochemical properties

Electrochemical properties of different block copolymers, donor and acceptor polymers were studied by cyclic voltammetry (CV).In the measurement, the polymer films were prepared by dispensing polymer chloroform solutions onto the working electrode at room temperature under a nitrogen atmosphere, and ferrocene was used as the internal reference. Relevant cyclic voltammograms of polymers are shown in Figure 5 and the corresponding data are summarized in Table 2. The covalently linked block copolymers exhibited quasi-reversible oxidation potentials. Their HOMO levels were calculated from the onset of oxidation curves, while the LUMO calculated from the difference between HOMO and optical bandgap. As shown from the energy diagram of Figure 5c, it is interesting that both the HOMO and LUMO levels of the block copolymers are located in between P3HT and PBIT2. By sequentially decreasing the donor or increasing the acceptor block weight content, gradual lowering of HOMO and LUMO from P3HT, BCP1-1, 1-2, 1-3 (or 2-1, 2-2, 2-3) and PBIT2 can be observed, which was regularly influenced by the conjugation and D-A interaction between the donor and accepter chain.

Table 2 Electrochemical and optical properties of polymers.

Polymer	λ_{max}(nm)[a]	λ_{max}(nm)[b]	E_g[c] (eV)	HOMO[d] (eV)	LUMO[e] (eV)
P3HT-1	453	555	1.85	5.07	3.22
BCP1-1	456	509	1.63	5.27	3.64
BCP1-2	456	508	1.61	5.33	3.72
BCP1-3	458	503	1.61	5.34	3.73
PBIT2	360,479,600	346,607	1.55	5.53	3.98
P3HT-2	453	555	1.83	5.05	3.22
BCP2-1	454	555	1.83	5.18	3.35
BCP2-2	456	547	1.61	5.20	3.59
BCP2-3	456	529	1.61	5.27	3.66

[a] Maximum absorption peak in dilute chloroform solution; [b] as-cast film from chloroform solution; [c] determined by UV-Vis absorption edge in film; [d] HOMO measured by CV; [e] LUMO calculated from the difference of HOMO and bandgap.

All-polymer solar cells

The potential application of block copolymer as a single-component active layer in all-polymer solar cells was investigated. Among all the as separated block copolymers, BCP1-1 with the most monomodal GPC curves, nearly the narrowest PDI of 1.23 and suitable P3HT weight ratio of 47 wt% was selected as the representatives. The device architecture is as follows: ITO/PEDOT: PSS/BCP1-1/Ca/Al. The current density voltage (*J*–*V*) curves of the fabricated all-polymer solar cells under 100 mW/cm^2 AM1.5G solar illuminations are shown in Figure 6. The open-circuit voltage (V_{oc}), short current (J_{sc}), fill factor (*FF*), and PCEs are summarized in Table 3. In general, the thermally annealed devices displayed a drastic improvement of J_{sc}, *FF* and PCE which may be attributed to thermally induced crystallization and enhanced phase-separated nano-structures of the active component resulted in enhancing charge generation and improving charge transport.[58] For example, the as-spun BCP1-1 gave the rather low PCE of 0.06% with V_{oc} of 0.25 V, J_{sc} of 0.83 mA/cm^2, and *FF* of 0.27. Thermal annealing resulted in an increase of V_{oc} and a dramatic improvement of the J_{sc}, and finally, the optimized PCE of 1.0% with V_{oc} of 0.43 V, J_{sc} of 5.29 mA/cm^2, and *FF* of 0.43, were achieved when the simple active layer was thermally annealed at 150°C. In addition to the thermal annealing conditions, other factors relating to device fabrication (e.g., solvents, additives, and thickness of layers) might also affect the photovoltaic performance,[59–63] and thus, we believe that further improvement of the PCEs of the BCP1-1 could be achieved by optimizing device fabrication conditions *via* the above mentioned factors.

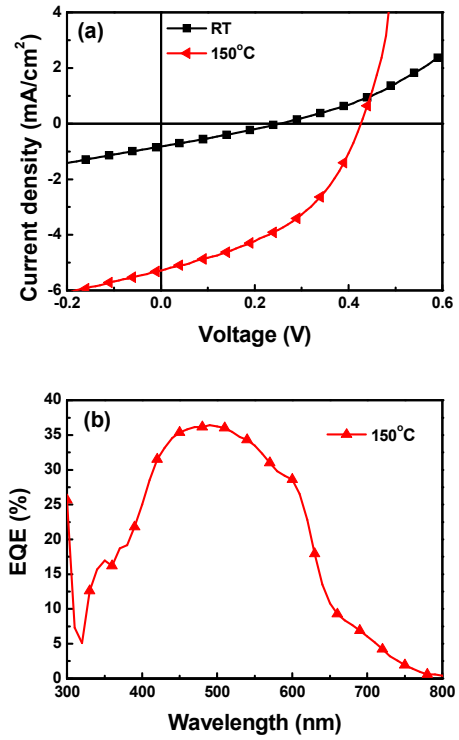

Fig. 6 *J*–*V* characteristics (a) and EQE curves (b) of the solar cells based on BCP1-1.

Table 3 Performance of all-polymer solar cell using the BCP1-1 system.

Device	V_{OC} (V)	J_{SC} (mA/cm^2)	FF	PCE_{max} (average) (%)
RT	0.25	0.83	0.27	0.06 (0.06±0.02)
150˚C	0.43	5.29	0.43	1.00 (0.96±0.07)

In order to study the charge transport properties of the block copolymers, the hole and electron mobility of the thermal annealed active film of BCP1-1 was measured by the space charge limited current (SCLC) method (Figure 7) according to literature reported procedures.[64-66] Hole-only and electron-

only diodes using the architectures of ITO/PEDOT:PSS/BCP1-1/Au for holes and Al/BCP1-1/Al for electrons were fabricated. The hole and electron mobility for BCP1-1 was measured to be 2.36×10^{-4} and 1.15×10^{-5} cm^2/Vs, respectively, with the hole-mobility one-order slightly higher than the electron-mobility. It should be mentioned that the charge transport properties of block copolymers have never been reported. The good and comparatively balanced charge transport characteristics of the block copolymers ensured efficient charge transport and charge collection in the single-component solar cell device, and thus to afford moderate device performance, which also provides the guidance of the promising future for fully-conjugated donor-acceptor block copolymers in the application of single-component solar cells.

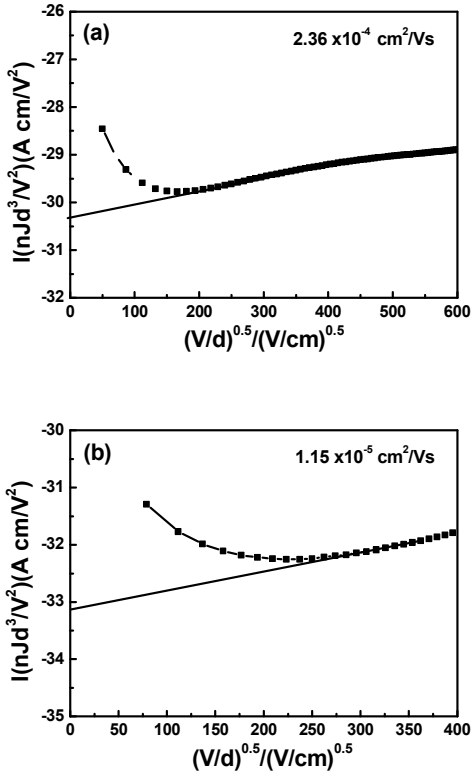

Fig. 7 *J*– *V* characteristics for (a) hole-only and (b) electron-only devices based on BCP1-1 film after annealing at 150°C.

Film morphologies

The effect of surface morphology on the photovoltaic performance of the BCP1-1 films was investigated by atomic force microscopy (AFM) measurement. Figure 8 shows the AFM images of the BCP1-1 film before and after thermal annealing. The root-mean square roughness of the as-cast and thermal annealing film was 3.69 and 5.40 nm, respectively. It can also be observed from Figure 8b and d, the thermally annealed block copolymer film exhibited coarsening and large domain size, which amplified the phase-separated bicontinuous interpenetrated network (Figure 8b), thus significantly increased the device photovoltaic performance.

Further evidence for enhanced phase separation of solid-state molecular organization of the block copolymers was conducted by X-ray diffraction (XRD) analysis. The sample of BCP1-1 thin film was prepared by drop-casting from chlorobenzene solution onto a glass substrate at ambient temperature or thermally annealed at 150°C for 10 minutes in nitrogen atmosphere. The XRD spectra of the block copolymers are shown in Figure 9. The diffraction pattern for both films exhibited two reflection sharp peaks which was attributed to P3HT and PBIT2 homopolyer respectively, indicating a retaining of the intrinsic crystalline characteristic to both blocks as well as distinct phase-separation between the donor P3HT and acceptor PPBIT2 in block copolymers. The prominent peak appeared at low angle of $2\theta = 5.4°$ corresponding to a d-spacing of 16.4 Å of the well-organized lamellar structure of *p*-type P3HT.[67] And the high angle exhibited at $2\theta = 21.4°$, corresponding to the π-π stacking between the *n*-type PBIT units with d-spacing of 4.1 Å, respectively.[37] It should be noted that the diffraction intensity attributing to the crystallization of P3HT was significantly enhanced after thermal annealing, suggesting amplified phase-separation between the donor and acceptor block and the well-ordered molecular arrangement in polymer film.

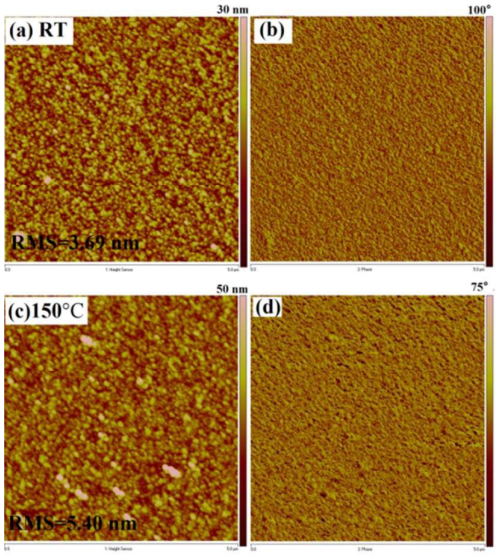

Fig. 8 AFM topography (left) and phase (right) images (5 μm × 5 μm) of BCP1-1film: (a, b) as-spun and (c, d) after annealing at 150°C.

Conclusion

In conclusion, fully conjugated D-A block copolymers P3HT-*b*-PBIT2 have been successfully synthesized through Stille coupling polycondensation in a one-pot reaction. Careful purification with preparative GPC were carried out to obtain various block copolymers with different P3HT donor and PBIT2 acceptor block lengths. It has been found that optical and electrochemical properties of D-A block copolymers are

strongly dependent on the combination ratio of the donor P3HT and acceptor PBIT2 segment. All-polymer solar cells with simple single-component active layer of P3HT-*b*-PBIT2 achieved a power conversion efficiency of 1.0%. These results demonstrated that fully conjugated D−A block copolymers are potentially applicable as single-component active materials, and more efficient photovoltaic performance can be achieved by optimization of chemical structures and the device fabrication conditions.

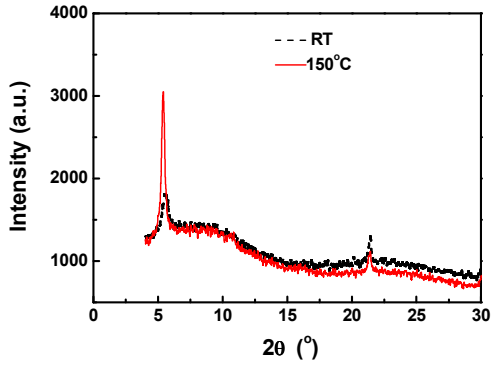

Fig. 9 XRD patterns of BCP1-1film: as-spun and annealed at 150°C.

Acknowledgements

We thank the National Natural Science Foundation of China (21304047), NSF of Jiangsu Province (13KJB430017) and Synergetic Innovation Center for Organic Electronics and Information Displays for financial support.

Notes and references

1 J. J. M. Halls, C. A. Walsh, N. C. Greenham, E. A. Marseglia, R. H. Friend, S. C. Moratti and A. B. Holmes, *Nature*, 1995, **376**, 498.
2 Y.-J. Hwang, B. A. E. Courtright, A. S. Ferreira, S. H. Tolbert and S. A. Jenekhe, *Adv. Mater*., 2015, **27**, 4578.
3 T.W. Holcombe, C. H. Woo, D. F. J. Kavulak, B. C. Thompson and J. M. J. Fr´echet, *J. Am. Chem. Soc*., 2009, **131**, 14160.
4 J. E. Anthony, A. Facchetti, M. Heeney, S. R. Marder and X. Zhan, *Adv. Mater*., 2010, **22**, 3876.
5 A. Facchetti, *Mater. Today,* 2013, **16**, 123.
6 J. Wang and T. Higashihara, *Polym. Chem*., 2013, **4**, 5513.
7 C. R. McNeill, A. Abrusci, I. Hwang, M. A. Ruderer, P. Muller-Buschbaum and N. C. Greenham, *Adv. Funct. Mater*., 2009, **19**, 3103.
8 R. Shikler, M. Chiesa and R. H. Friend, *Macromolecules*, 2006, **39**, 5393.
9 C. R. McNeill, B. Watts, L. Thomsen, W. J. Belcher, N. C. Greenham, P. C. Dastoor and H. Ade, *Macromolecules*, 2009, **42**, 3347.
10 S. Swaraj, C. Wang, H. Yan, B. Watts, J. Luning, C. R. McNeill and H. Ade, *Nano. Lett*., 2010, **10**, 2863.
11 E. Zhou, J. Cong, Q. Wei, K. Tajima, C. Yang and K. Hashimoto, *Angew. Chem. Int. Ed*., 2011, **50**, 2799.
12 M. Schubert, D. Dolfen, J. Frisch, S. Roland, R. Steyrleuthner, B. Stiller, Z. Chen, U. Scherf, N. Koch, A. Facchetti and D. Neher, *Adv. Energy Mater*., 2012, **2**, 369.
13 J. R. Moore, S. Albert-Seifried, A. Rao, S. Massip, B. Watts, D. J. Morgan, R. H. Friend, C. R. McNeill and H. Sirringhaus, *Adv. Energy Mater*., 2011, **1**, 230.
14 E. S. Joanna, H. Ximin and W. T. S. Hucka, *Nano. Today,* 2010, **5**, 231.
15 G. Yu, J. Gao, J. C. Hummelen, F. Wudl and A. J. Heeger, *Science,* 1995, **270**, 1789.
16 D. Mori, H. Benten, J. Kosaka, H. Ohkita, S. Ito, and K. Miyake, *ACS Appl. Mater. Inter*., 2011, **3**, 2924.
17 M. Qian, R. Zhang, J. Hao, W. Zhang, Q. Zhang, J. Wang, Y. Tao, S. Chen, J. Fang and W. Huang, *Adv. Mater*., 2015, **27**, 3546.
18 M. Schubert, D. Dolfen, J. Frisch, S. Roland, R. Steyrleuthner, B. Stiller, Z. Chen, U. Scherf, N. Koch, A. Facchetti and D. Neher, *Adv. Energy Mater*., 2012, **2**, 369.
19 W. Ma, C. Yang, X. Gong, K. Lee and A. J. Heeger, *Adv. Funct. Mater*., 2005, **15**, 1617.
20 J. Peet, J. Y. Kim, N. E. Coates, W. L. Ma, D. Moses, A. J. Heeger and G. C. Bazan, *Nat. Mater.*, 2007, **6**, 497.
21 H. Xin, X. Guo, G. Ren, M. D. Watson and S. A. Jenekhe, *Adv. Energy Mater*., 2012, **2**, 575.
22 Y. Zhou, T. Kurosawa, W. Ma, Y. Guo, L. Fang, K. Vandewal, Y. Diao, C. Wang, Q. Yan, J. Reinspach, J. Mei, A. L. Appleton, G. I. Koleilat, Y. Gao, S. C. B. Mannsfeld, A. Salleo, H. Ade, D. Zhao and Z. Bao, *Adv. Mater.,* 2014, **26**, 3767.
23 F. S. Bates and G. H. Fredrickson, *Annu. Rev. Phys. Chem.,* 1990, **41**, 525.
24 S. Ullrich, G. Rea and K. Nls, *Acc. Chem. Res.,* 2008, **41**, 1086.
25 M. J. Robb, S. Y. Ku and C. J. Hawker, *Adv. Mater.,* 2013, **25**, 5686.
26 L. J. Bu, X. Y. Guo, B. Yu, Y. Qu, Z. Y. Xie, D. H. Yan, Y. H. Geng and F. S. Wang, *J. Am. Chem. Soc.,* 2009, **131**, 13242.
27 S. Wang, Y. Guo, J. Yang, Y. Tao and W. Huang, *Chin. J. Chem*., 2015, **33**, 865.
28 S.-Y. Ku, M. A. Brady, N. D. Treat, J. E. Cochran, M. J. Robb, E. J. Kramer, M. L. Chabinyc and C. J. Hawker, *J. Am. Chem. Soc*., 2012, **134**, 16040.
29 C. Guo, Y.-H. Lin, M. D. Witman, K. A. Smith, C. Wang, A. Hexemer, J. Strzalka, E. D. Gomez, and R. Verduzco, *Nano. Lett.,* 2013, **13**, 2957.
30 M. Sommer, H. Komber, S. Huettner, R. Mulherin, P. Kohn, N. C. Greenham and W. T. S. Huck, *Macromolecules,* 2012, **45**, 4142.
31 Y.-H. Lin, K. A. Smith, C. N.Kempf and R.Verduzco, *Polym. Chem*., 2013, **4**, 229.
32 R. C. Mulherin, S. Jung, S. Huettner, K. Johnson, P. Kohn, M. Sommer, S. Allard, U. Scherf and N. C. Greenham, *Nano. Lett*., 2011, **11**, 4846.
33 K. Nakabayashi and H. Mori, *Macromolecules,* 2012, **45**, 9618.
34 J. W. Mok, Y.-H. Lin, K. G. Yager, A. D. Mohite, W. Nie, S. B. Darling, Y. Lee, E. Gomez, D. Gosztola, R. D. Schaller and R. Verduzco, *Adv. Funct. Mater.,* 2015, DOI: 10.1002/adfm.201502623.
35 H. Kuang, M. J. Janik and E. D. Gomez, *J. Polym. Sci. Part B: Polym. Phys.*, 2015, **53**, 1224.
36 K. Nakabayashi and H. Mori, *J. Nanomater.*, 2015, **2015**, 1.
37 R. J. Ono, A. D. Todd, Z. Hu, D. A. V. Bout and C. W. Bielawski, *Macromol. Rapid Commun.,* 2014, **35**, 204.
38 Q. Zhang, A. Cirpan, T. P. Russell and T. Emrick, *Macromolecules*, 2009, **42**, 1079.
39 Y. Tao, B. McCulloch, S. Kim and R. A. Segalman, *Soft. Matter.*, 2009, **5**, 4219.
40 S. Rajaram, P. B. Armstrong, B. J. Kim and J. M. J. Fréchet, *Chem.Mater.,* 2009, **21**, 1775.

41 M. Sommer, A. S. Lang and M. Thelakkat, *Angew. Chem. Int. Ed*., 2008, **47**, 7901.
42 S. Huettner, J. M. Hodgkiss, M. Sommer, R. H. Friend, U. Steiner and M. Thelakkat, *J. Phys. Chem. B,* 2012, **116**, 10070.
43 R. H. Lohwasser, G. Gupta, P. Kohn, M. Sommer, A. S. Lang, T. Thurn-Albrecht and M. Thelakkat, *Macromolecules*, 2013, **46**, 4403.
44 G. Gupta, C. R. Singh, R. H. Lohwasser, M. Himmerlich, S. Krischok, P. Muller-Buschbaum, M. Thelakkat, H. Hoppe and T. Thurn-Albrecht, *ACS Appl. Mater. Interfaces*, 2015, **7**, 12309.
45 X. Zhang, Z. Lu, L. Ye, C. Zhan, J. Hou, S. Zhang, B. Jiang, Y. Zhao, J. Huang, S. Zhang, Y. Liu, Q. Shi, Y. Liu and J. Yao, *Adv.Mater.,* 2013, **25**, 5791.
46 A. F. Lv, S. R. Puniredd, J. H. Zhang, Z. B. Li, H. F. Zhu, W. Jiang,H. L. Dong, Y. D. He, L. Jiang, Y. Li, W. Pisula, Q. Meng, W. P. Hu and Z. H. Wang, *Adv. Mater*., 2012, **24**, 2626.
47 M. C. R. Delgado,E.-G. Kim, D. A. da Silva Filho and J.-L. Brédas, *J. Am. Chem. Soc*., 2010, **132**, 3375.
48 R. Schmidt, J. H. Oh, Y.-S. Sun, M. Deppisch, A.-M. Krause, K. Radacki, H. Braunschweig, M. Könemann, P. Erk, Z. Bao and F. Würthner, *J. Am. Chem. Soc*., 2009, **131**, 6215.
49 Z. An, J. Yu, S. C. Jones, S. Barlow, S. Yoo, B. Domercq, P. Prins, L. D. A. Siebbeles, B. Kippelen and S. R. Marder, *Adv. Mater.,* 2005, **17**, 2580.
50 B. A. Jones, M. J. Ahrens, M.-H. Yoon, A. Facchetti, T. J. Marks and M. R. Wasielewski, *Angew. Chem. Int. Ed.,* 2004, **43**, 6363.
51 J. J. Dittmer, E. A. Marseglia and R. H. Friend, *Adv. Mater.,* 2000, **12**, 1270.
52 Y. Guo, Y. Jin and Z. Su, *Polym. Chem.,* 2012, **3**, 861.
53 C. R. McNeill, J. J. M. Halls, R. Wilson, G. L. Whiting, S. Berkebile, M. G. Ramsey, R. H. Friend and N. C. Greenham, *Adv. Funct. Mater.,* 2008, **18**, 2309.
54 J. Qu, B. Gao, H. Tian, X. Zhang, Y. Wang, Z. Xie, H. Wang, Y. Geng and F. Wang, *J. Mater. Chem. A,* 2014, **2**, 3632.
55 L. J. Bu, X. Y. Guo, B. Yu, Y. Qu, Z. Y. Xie, D. H. Yan, Y. H. Geng and F. S. Wang, *J. Am. Chem. Soc.,* 2009, **131**, 13242.
56 R. Verduzco, I. Botiz, D. L. Pickel, S. M Kilbey, K. Hong, E. Dimasi and S. B. Darling, *Macromolecules,* 2011, **44**, 530.
57 S. Wang, J. Yang, Z. Zhang, Y. Hu, X. Cao, H. Li, Y. Tao, Y. Li and W. Huang, *RSC Adv.*, 2015, **5**, 68192.
58 W. L. Ma, C. Y. Yang, X. Gong, K. Lee and A. J. Heeger, *Adv. Funct. Mater.,* 2005, **15** 1617.
59 E. Zhou, J. Cong, Q. Wei, K. Tajima, C. Yang and K. Hashimoto, *Angew. Chem. Int. Ed*., 2011, **123**, 2851.
60 J. R. Moore, S. Albert-Seifried, A. Rao, S. Massip, B. Watts, D. J. Morgan, R. H. Friend, C. R. McNeill and H. Sirringhaus, *Adv. Energy Mater.,* 2011, **1**, 230.
61 D. Mori, H. Benten, J. Kosaka, H. Ohkita, S. Ito and K. Miyake, *ACS Appl. Mater. Interfaces*, 2011, **3**, 2924.
62 M. Schubert, D. Dolfen, J. Frisch, S. Roland, R. Steyrleuthner, B. Stiller, Z. Chen, U. Scherf, N. Koch, A. Facchetti and D Neher, *Adv. Energy Mater*., 2012, **2**, 369.
63 D. Mori, H. Benten, H. Ohkita, S. Ito and K.Miyake, *ACS Appl. Mater. Interfaces*, 2012, **4**, 3325.
64 G. G. Malliaras, J. R. Salem, P. J. Brock and C. Scott, *Phys. Rev. B: Condens. Matter Mater. Phys*., 1998, **58**, 13411.
65 P. Cheng, Y. Li and X. Zhan, *Energy Environ. Sci*., 2014, **7**, 2005.
66 M. Koppe, H. J. Egelhaaf, G. Dennler, M. C. Scharber,C. J. Brabec, P. Schilinsky and C. N. Hoth, *Adv. Funct. Mater*., 2010, **20**, 338.
67 X. Yu, H. Yang, S. Wu, Y. Geng and Y. Han, *Macromolecules*, 2012, **45**, 266.

Fully conjugated block copolymers for single-component solar cells: synthesis, purification, and characterization

Shifan Wang, Qingqing Yang, Youtian Tao,* Yan Guo, Jie Yang, Yanan Liu, Lingyun Zhao, Zhiyuan Xie,* Wei Huang*

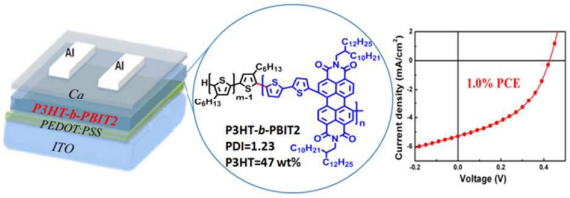

All-polymer solar cells using the preparative GPC separated block copolymer P3HT-*b*-PBIT2 as simple active layer shows a power conversion efficiency of 1.0%.